NEW THERMONUCLEAR REACTION RATE EQUATIONS FOR RADIATIVE NEUTRON CAPTURE

Vinay Singh[a,b,†], Joydev Lahiri[a,‡], D.N. Basu[a,b,§]

[a]Variable Energy Cyclotron Centre
1/AF Bidhan Nagar, Kolkata 700064, India
[b]Homi Bhabha National Institute
Training School Complex, Anushakti Nagar, Mumbai 400085, India

(Received February 12, 2021; accepted May 10, 2021)

The radiative neutron capture reaction rates for $^{6}\mathrm{Li}(n,\gamma)^{7}\mathrm{Li}$, $^{10}\mathrm{B}(n,\gamma)^{11}\mathrm{B}$, $^{12}\mathrm{C}(n,\gamma)^{13}\mathrm{C}$ and $^{14}\mathrm{N}(n,\gamma)^{15}\mathrm{N}$ have been studied at very low energies which are of interest for nuclear astrophysics. The rates of these reactions have remained independent of temperature so far. The temperature dependence of the thermonuclear reaction rates has been explored within the statistical model. Apart from the compound nuclear contribution, the pre-equilibrium as well as the direct effects have been taken into account. The corresponding Maxwellian-averaged thermonuclear reaction rates of relevance in astrophysical plasmas at temperatures in the range from 10^{6}K to 10^{10}K have been calculated. New reaction rates have been obtained for $^{6}\mathrm{Li}(n,\gamma)^{7}\mathrm{Li}$, $^{10}\mathrm{B}(n,\gamma)^{11}\mathrm{B}$, $^{12}\mathrm{C}(n,\gamma)^{13}\mathrm{C}$ and $^{14}\mathrm{N}(n,\gamma)^{15}\mathrm{N}$. For $^{6}\mathrm{Li}(n,\gamma)^{7}\mathrm{Li}$, an analytical expression as a function of T_9 has been obtained.

DOI:10.5506/APhysPolB.52.453

1. Introduction

The astrophysical thermonuclear reactions generate energy that makes stars shine. These are also responsible for the synthesis of the elements in stars. The interstellar medium is enriched with the nuclear ashes when stars dislodge a portion of their content via various channels. These processes provide the elementary units for the creation of new stars as well as planets and life itself. The 'nucleosynthesis' which is a theory of production of elements is exceptionally successful in representing these nuclear processes in stars that are located quite far away from us in space and time. The process

† vsingh@vecc.gov.in
‡ joy@vecc.gov.in
§ dnb@vecc.gov.in

of synthesis of the elements can be broadly classified into two categories: the primordial or Big Bang Nucleosynthesis and the stellar nucleosynthesis. As the name suggests, the primordial nucleosynthesis refers to what happened at the beginning of the Universe when light elements such as D, T, ^{3,4}He, ^{6,7}Li and ^{7}Be were synthesized while stellar nucleosynthesis occurs in stars and causes synthesis of heavier elements. It is also worth attention how the nucleosynthesis prognosticates these processes on the basis of quantum mechanical properties of atomic nuclei. The generation of nuclear energy in stars, nucleosynthesis and various other issues at the crossway of nuclear physics and astrophysics compose the science of nuclear astrophysics. Similar to most areas of physics, it involves both experimental and theoretical activities.

The nuclear reaction cross sections and its convolution with the Maxwell–Boltzmann distribution of energies are important for modeling many physical phenomena occurring under extreme conditions [1–3]. Such environments of very high temperature or density exist in main-sequence stars and compact stars which are in final stages of their evolutionary development. The exothermic nuclear fusion drives nuclear explosions in the surface layers of the accreting white dwarfs (nova events), in the cores of massive accreting white dwarfs (type Ia supernovae) [4, 5], and in the surface layers of accreting neutron stars (type I X-ray bursts and superbursts [6–9]). All these astrophysical processes require precise knowledge of nuclear reaction rates obtained by convoluting cross sections with the Maxwell–Boltzmann distribution of energies. The Maxwellian-averaged thermonuclear reaction rate per particle pair $\langle \sigma v \rangle$ at temperature T can be represented by the integral [10–12] described below

$$\langle \sigma v \rangle = \left[\frac{8}{\pi m (kT)^3} \right]^{1/2} \int \sigma(E) E \exp\left(\frac{-E}{kT} \right) \mathrm{d}E \,, \tag{1}$$

where v is the relative velocity, E is the energy in the centre-of-mass system, k and m are the Boltzmann constant and the reduced mass of the reacting nuclei, respectively. Therefore, the reaction rate between two nuclei can be written as $r_{12} = \frac{n_1 n_2}{1+\delta_{12}} \langle \sigma v \rangle$, where n_1 and n_2 are the number densities of nuclei of types 1 and 2. The Kronecker delta δ_{12} prevents double counting in the case of identical particles.

Several works [13–17] regarding reaction rates have been done in the past. Except for a few neutron-induced reactions, all other reaction rates have temperature dependences. At thermal energies, the neutron absorption cross section shows an approximate $1/v$ behavior. Hence, using $\sigma(E) \propto E^{-1/2}$ in Eq. (1) immediately shows that the reaction rates are approximately constant with respect to the temperature at low energies. However, this fact is true for thermal neutrons ($\sim$ 0.025 eV) only with energies of the

order of eV and below. However, at energies of astrophysical interest, the neutron-induced reaction cross sections can be given by $\sigma(E) = \frac{R(E)}{v}$ [18], where $R(E)$ is a gently varying function of energy [19] which is similar to the astrophysical S-factor, and one expects $\langle \sigma v \rangle$ to be dependent on temperature. Since $^{6}\mathrm{Li}(n,\gamma)^{7}\mathrm{Li}$, $^{10}\mathrm{B}(n,\gamma)^{11}\mathrm{B}$, $^{12}\mathrm{C}(n,\gamma)^{13}\mathrm{C}$ and $^{14}\mathrm{N}(n,\gamma)^{15}\mathrm{N}$ are the reactions with rates independent of temperature, it attracted special attention for further investigation of the temperature dependence.

2. Theoretical formalism

The thermonuclear reaction rates can be obtained by convoluting fusion cross sections with the Maxwell–Boltzmann distribution of energies. These cross sections can vary by several orders of magnitude across the required energy range. The low-energy fusion cross sections σ, some of which are not sufficiently well-known, can be obtained from laboratory experiments. However, there are cases, in particular involving the weak interaction such as the basic $p + p$ fusion to deuterium in the solar p–p chain, where no experimental data are available and one completely relies on theoretical calculations [10]. The predictions of the thermonuclear reaction rates calculated theoretically depend upon various approximations used. Several factors affect the cross-section values measured experimentally. We need to account for the Maxwellian-averaged thermonuclear reaction rates in the network calculations used in the primordial and stellar nucleosynthesis.

The reaction rates used in the Big Bang Nucleosynthesis (BBN) reaction network have temperature dependences except for $^{6}\mathrm{Li}(n,\gamma)^{7}\mathrm{Li}$, $^{10}\mathrm{B}(n,\gamma)^{11}\mathrm{B}$, $^{12}\mathrm{C}(n,\gamma)^{13}\mathrm{C}$ and $^{14}\mathrm{N}(n,\gamma)^{15}\mathrm{N}$ which are constant with respect to temperature. The computer code TALYS [20] allows a comprehensive astrophysical reaction rate calculations apart from other nuclear physics calculations. To a good approximation, in the interior of stars, the assumption of a thermodynamic equilibrium holds and nuclei exist both in the ground and excited states. This assumption along with cross sections calculated from the compound nucleus model for various excited states facilitates Maxwellian-averaged reaction rates. For stellar evolution models, this is quite an important input. The nuclear reaction rates are generally evaluated using the statistical model [21, 22] and astrophysical calculations mostly use these reaction rates. Stellar reaction rate calculations have been routinely done in past [23, 24]. However, TALYS has extended these Hauser–Feshbach statistical model [25] calculations by adding some new and important features. Apart from coherent inclusion of fission channel, it also includes a reaction mechanism that occurs before equilibrium is reached, multi-particle emission, competition among all open channels, width fluctuation corrections in detail, coupled channel description in the case of deformed nuclei and level

densities that are parity-dependent. The nuclear models are also normalized for available experimental data using separate approaches such as on photo-absorption data, the E1 resonance strength or on s-wave spacings, the level densities.

In the low-energy domain, a compound nucleus is formed by the fusion of the projectile and the target nuclei. While the total energy $E^{\rm tot}$ is fixed from energy conservation, the total spin J and parity Π can have a range of values. The reaction obeys the following conservation laws:

$$\begin{aligned} E_a + S_a &= E_{a'} + E_x + S_{a'} = E^{\rm tot}\,, \qquad \text{energy conservation}\,,\\ s + I + l &= s' + I' + l' = J\,, \qquad \text{angular momentum conservation}\,,\\ \pi_0 \Pi_0 (-1)^l &= \pi_f \Pi_f (-1)^{l'} = \Pi\,, \qquad \text{parity conservation}\,. \end{aligned}$$

The formula for binary cross section, assuming the compound nucleus model, is given by

$$\begin{aligned} \sigma^{\rm comp}_{\alpha\alpha'} &= D^{\rm comp}\frac{\pi}{k^2}\sum_{J=\mathrm{mod}(I+s,1)}^{l_{\max}+I+s}\ \sum_{\Pi=-1}^{1}\frac{2J+1}{(2I+1)(2s+1)}\\ &\times \sum_{j=|J-I|}^{J+I}\ \sum_{l=|j-s|}^{j+s}\ \sum_{j'=|J-I'|}^{J+I'}\ \sum_{l'=|j'-s'|}^{j'+s'}\delta_\pi(\alpha)\delta_\pi\left(\alpha'\right)\\ &\times \frac{T^J_{\alpha l j}(E_a)\left\langle T^J_{\alpha' l' j'}\left(E_{a'}\right)\right\rangle}{\sum_{\alpha'',l'',j''}\delta_\pi\left(\alpha''\right)\left\langle T^J_{\alpha'' l'' j''}\left(E_{a''}\right)\right\rangle} W^J_{\alpha l j \alpha' l' j'}\,, \end{aligned} \tag{2}$$

where

E_a = the energy of the projectile,

l = the orbital angular momentum of the projectile,

s = the spin of the projectile,

j = the total angular momentum of the projectile,

π_0 = the parity of the projectile,

$$\delta_\pi(\alpha) = \begin{cases} 1 & \text{if } \ (-1)^l \pi_0 \Pi_0 = \Pi \\ 0 & \text{otherwise} \end{cases}\,,$$

α = the designation of the channel for the initial projectile–target system: $\alpha = \{a,\ s,\ E_a,\ E^0_x,\ I,\ \Pi_0\}$, where a and E^0_x are the type of the projectile and the excitation energy (which is zero usually) of the target nucleus, respectively,

$l_{\max}$ = the maximum l-value of the projectile,

S_a = the separation energy,

$E_{a'}$ = the energy of the ejectile,

l' = the orbital angular momentum of the ejectile,

s' = the spin of the ejectile,

j' = the total angular momentum of the ejectile,

π_f = the parity of the ejectile,

$$\delta_\pi(\alpha') = \begin{cases} 1 & \text{if } (-1)^{l'}\pi_f \Pi_f = \Pi \\ 0 & \text{otherwise} \end{cases},$$

α' = the designation of channel for the ejectile–residual nucleus final system:

$\alpha' = \{a',\ s',\ E_{a'},\ E_x,\ I',\ \Pi_f\}$, where a' and E_x are the type of the ejectile and the residual nucleus excitation energy, respectively,

I = the spin of target nucleus,

Π_0 = the parity of target nucleus,

I' = the spin of residual nucleus,

Π_f = the parity of residual nucleus,

J = the total angular momentum of the compound system,

Π = the parity of the compound system,

D^{comp} = the depletion factor so as to take into account for pre-equilibrium and direct effects,

k = the wave number of the relative motion,

T = the transmission coefficient,

W = the correction factor for width fluctuation (WFC).

The velocities of both the targets and projectiles obey the Maxwell–Boltzmann distributions corresponding to ionic plasma temperature T at the site. The astrophysical nuclear reaction rate can be calculated by folding the Maxwell–Boltzmann energy distribution for energies E at the given temperature T with the cross section given by Eq. (2). Additionally, target nuclei exist both in ground and excited states. The relative populations of various energy states of nuclei with excitation energies E_x^μ and spins I^μ in thermodynamic equilibrium follows the Maxwell–Boltzmann distribution. In order to distinguish between different excited states the superscript μ is used along with the incident α channel in the formulas that follow. Taking due account of various target nuclei excited state contributions, the effective nuclear reaction rate in the entrance channel $\alpha \to \alpha'$ can be finally expressed as

$$N_{\mathrm{A}}\langle\sigma v\rangle^{*}_{\alpha\alpha'}(T) = \left(\frac{8}{\pi m}\right)^{1/2} \frac{N_{\mathrm{A}}}{(kT)^{3/2}G(T)} \times \int_0^\infty \sum_\mu \frac{(2I^\mu+1)}{(2I^0+1)} \sigma^\mu_{\alpha\alpha'}(E) E \exp\left(-\frac{E+E^\mu_x}{kT}\right) \mathrm{d}E\,, \quad (3)$$

where N_{A} is the Avogadro number which is equal to 6.023×10^{23}, k and m are the Boltzmann constant and the reduced mass in the α channel, respectively, and

$$G(T) = \sum_\mu \frac{(2I^\mu+1)}{(2I^0+1)} \exp\left(\frac{-E^\mu_x}{kT}\right)$$

is the temperature-dependent normalized partition function. By making use of the reciprocity theorem [26], the reverse reaction cross sections or rates can also be estimated.

3. Calculations and results

All the reaction rates used in the BBN reaction network have temperature dependences except for a few such as $^6\mathrm{Li}(n,\gamma)^7\mathrm{Li}$, $^{10}\mathrm{B}(n,\gamma)^{11}\mathrm{B}$, $^{12}\mathrm{C}(n,\gamma)^{13}\mathrm{C}$ and $^{14}\mathrm{N}(n,\gamma)^{15}\mathrm{N}$. The experimental status is that only one direct measurement of the $^6\mathrm{Li}(n,\gamma)^7\mathrm{Li}$ cross sections has been performed [27] at stellar energies. The Malaney–Fowler reaction rate [14] for $^6\mathrm{Li}(n,\gamma)^7\mathrm{Li}$ in the BBN reaction network calculations has been taken as 5.10×10^3 $\mathrm{cm^3s^{-1}mol^{-1}}$ which is constant with respect to temperature. In a recent calculation [28] it was found to be $(8.5\pm1.7)\times10^3$ $\mathrm{cm^3s^{-1}mol^{-1}}$, where the error resulted from the uncertainties of spectroscopic factors and scattering potential depth. The astrophysical reaction rate was found to be higher by a factor of 1.7 than the value adopted in previous reaction network calculations [29–31]. For the reactions $^{10}\mathrm{B}(n,\gamma)^{11}\mathrm{B}$, $^{12}\mathrm{C}(n,\gamma)^{13}\mathrm{C}$ and $^{14}\mathrm{N}(n,\gamma)^{15}\mathrm{N}$, rates constants with respect to temperature given by 6.62×10^4, 4.50×10^2 and 9.94×10^3 $\mathrm{cm^3s^{-1}mol^{-1}}$, respectively [32], have been used.

The radiative neutron capture cross section varies inversely as velocity in the range of thermal energies. At these energies, the feature of $\sigma(E)\propto E^{-1/2}$ leads to approximate constancy of thermonuclear reaction rates with respect to plasma temperature. However, above thermal energies, especially in the domain of astrophysics, the neutron-induced reaction cross section deviates from the $1/v$ law and rather follows the dependence given by $\sigma(E)=\frac{R(E)}{v}$ [18]. Thus, it is expected that $\langle\sigma v\rangle$ has to have a temperature dependence. As discussed earlier, all the thermonuclear reaction rates do have temperature dependences except for a few neutron-induced reactions. These rates have remained independent of temperature so far and, therefore, attracted special attention for further investigation of their temperature dependences.

Due to the reason that the cross sections involved in nuclear astrophysics are very low, one of the main problems is the extrapolation of the data available down to very low energies. For this purpose, various models, such as microscopic approaches or the potential model, are extensively used. These are, in general, not very flexible to describe the data with reasonably good accuracy. Obviously, the polynomial approximation is the simplest way to extrapolate these data [15]. Usually, this method is used to investigate electron screening effects, where the cross section between bare nuclei is obtained from extrapolating the high-energy data by a polynomial approximation. Though very simple, the polynomial approximation is not based upon a rigorous analysis of the energy dependence of the cross section, and may induce significant inaccuracies. As mentioned in the previous section, a more rigorous approach has been used here.

The statistical model can be applied for the majority of nuclear reactions in astrophysics [23]. This is appropriate only if the level density in the concerned energy window near the peak of the projectile energy distribution is substantially high to justify a statistical treatment. The estimated critical level density is about 5 to 10 MeV^{-1} [21]. Moreover, the compound nucleus picture would provide a good description only when the energy of the incident particle is low enough. While the latter point is mostly satisfied in astrophysical environments, the level density criterion may not. It may fall below the critical value for very neutron-rich or proton-rich isotopes near the drip lines with correspondingly low separation energies and in certain nuclei lighter than Fe, at shell closures. In these cases, direct capture or single resonances contributions will become significant and have to be treated individually. In the present calculations, these effects have been taken into consideration.

The reaction rates for the reactions $^{6}\mathrm{Li}(n,\gamma)^{7}\mathrm{Li}$, $^{10}\mathrm{B}(n,\gamma)^{11}\mathrm{B}$, $^{12}\mathrm{C}(n,\gamma)^{13}\mathrm{C}$ and $^{14}\mathrm{N}(n,\gamma)^{15}\mathrm{N}$ have been calculated theoretically using the TALYS [20] code. Although in these reactions the nuclei involved are light, the results of the calculations are expected to be reasonable, particularly as the reaction being induced by low-energy neutrons and not by charged particles [16] implying dominant contributions from a compound nuclear reaction. Moreover, apart from the compound nuclear contribution, TALYS accounts for the pre-equilibrium and the direct effects as well. However, the pre-equilibrium effects do not play any role for $^{6}\mathrm{Li}(n,\gamma)^{7}\mathrm{Li}$ at energies below the ^{7}Li neutron separation energy of 7.25 MeV. The results of the calculations for $^{6}\mathrm{Li}(n,\gamma)^{7}\mathrm{Li}$ reaction rate in units of $\mathrm{cm}^{3}\mathrm{s}^{-1}\mathrm{mol}^{-1}$ as a function of temperature T_9 generated from the TALYS code have been presented in Table I, whereas for the rest of the reactions, $^{10}\mathrm{B}(n,\gamma)^{11}\mathrm{B}$, $^{12}\mathrm{C}(n,\gamma)^{13}\mathrm{C}$ and $^{14}\mathrm{N}(n,\gamma)^{15}\mathrm{N}$, the rates have been found to be approximately constant given by $5.3318 \times 10^{3} \pm 8.67$, $2.8749 \times 10^{3} \pm 5.81$ and

$4.2081 \times 10^4 \pm 3.97 \times 10^1$ $\mathrm{cm^3 s^{-1} mol^{-1}}$, respectively. In Table I, the reaction rates with the asterisk (*) mark are the results of calculations for the reaction $^6\mathrm{Li}(n,\gamma)^7\mathrm{Li}$ with the direct capture effects included. Inclusion of the direct capture effects also modify the reaction rates (which still remain approximately independent of temperature) for $^{10}\mathrm{B}(n,\gamma)^{11}\mathrm{B}$, $^{12}\mathrm{C}(n,\gamma)^{13}\mathrm{C}$ and $^{14}\mathrm{N}(n,\gamma)^{15}\mathrm{N}$ to $2.2014 \times 10^5 \pm 1.76 \times 10^2$, $4.0473 \times 10^4 \pm 3.72 \times 10^1$ and $6.8963 \times 10^4 \pm 2.28 \times 10^1$ $\mathrm{cm^3 s^{-1} mol^{-1}}$, respectively. However, even when the direct capture effects are included, the cross-section values for the $^6\mathrm{Li}(n,\gamma)^7\mathrm{Li}$ reaction are underestimated, the reason being that the Hauser–Feshbach theory is not suitable for such a low-mass system with a low-level density, as mentioned earlier. The ^{7}Li spectrum, however, presents five levels within an interval of ~ 6 MeV above the $^6\mathrm{Li}+n$ threshold. This corresponds to a level density of less that $\sim 1/\mathrm{MeV}$. Therefore, the code TALYS is not very suitable to obtain reliable results for such a light system. The $^6\mathrm{Li}(n,\gamma)^7\mathrm{Li}$ neutron radiative capture reaction cross sections can be obtained reliably from the Gamow shell model formulated in the coupled-channel representation [33].

TABLE I

Reaction rate in units of $\mathrm{cm^3 s^{-1} mol^{-1}}$ for the $^6\mathrm{Li}(n,\gamma)^7\mathrm{Li}$ reaction as a function of temperature T_9 (expressed in units of 10^9 K) generated from TALYS. The reaction rates with the asterisk (*) mark are the results of calculations with the direct capture effects included.

T_9	Reaction rate	Reaction rate*	T_9	Reaction rate	Reaction rate*	T_9	Reaction rate	Reaction rate*
0.0001	408.43	889.21	0.3	436.44	1006.48	2.5	824.89	1745.76
0.0005	440.24	970.66	0.4	466.02	1057.18	3.0	883.00	1854.84
0.001	423.09	940.34	0.5	492.41	1102.93	3.5	936.22	1948.29
0.005	414.78	949.75	0.6	516.58	1145.66	4.0	985.55	2028.21
0.01	392.78	912.98	0.7	539.18	1186.48	5.0	1074.75	2154.22
0.05	369.81	889.08	0.8	560.55	1225.87	6.0	1153.17	2244.31
0.1	375.42	902.00	0.9	580.88	1264.05	7.0	1222.50	2308.07
0.15	388.01	923.75	1.0	600.31	1301.12	8.0	1284.74	2353.98
0.2	403.71	950.52	1.5	686.76	1471.30	9.0	1342.36	2389.40
0.25	420.29	978.86	2.0	760.28	1618.70	10.0	1397.99	2420.41

4. Analytical parametrization of reaction rates

In order to provide analytical parametrization of reaction rate, the results presented in Table I have been fitted quite accurately as a function of T_9. The parameterization adapted for this neutron-induced reaction is

$$N_{\mathrm{A}}\langle\sigma v\rangle(T) = a_0\left(1 + \sum_{i=1}^{N} a_i T_9^i\right) \tag{4}$$

which provides an excellent fit to the calculated values as evident from Fig. 1. The values of the parameters obtained are $a_0 = 387.75 \pm 0.95$, $a_1 = 0.5659 \pm 0.0059$, $a_2 = (-0.52746 \pm 0.01586) \times 10^{-1}$ and $a_3 = (0.22354 \pm 0.01168) \times 10^{-2}$. For the results of calculations with the direct capture effects included, these parameters get modified to $a_0 = 897.394 \pm 0.79$, $a_1 = 0.4910 \pm 0.0020$, $a_2 = (-0.51663 \pm 0.00542) \times 10^{-1}$ and $a_3 = (0.19537 \pm 0.00393) \times 10^{-2}$. The errors in the fitted parameters are calculated from the correlation matrix in the final stage of the fitting procedure when changes in the fitted parameters by amounts equal to the corresponding uncertainties in the fitted parameters cause changes in the corresponding quantity by less than the stipulated value. Thus, large uncertainty in a fitted parameter implies that the hypersurface is rather flat with respect to that parameter. We also find that the contributions from terms containing higher orders of T_9 are insignificant. Hence, terms only up to third order in T_9 have been retained in Eq. (4). Moreover, any other form such as that provided in [17] for charged-particle-induced reactions could not be fitted with even a reasonable value of chi-square per degrees of freedom.

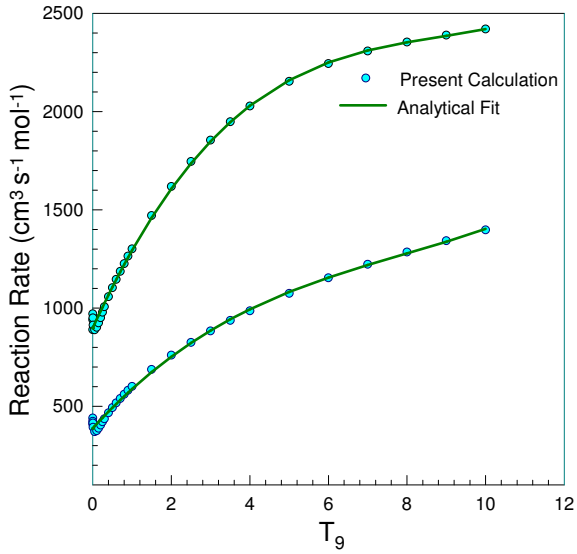

Fig. 1. Plot of reaction rate as a function of temperature T_9. The dots represent results of the present calculations while the continuous line represents the fit to it. The upper curve corresponds to the results of calculations with the direct capture effects included.

The plot of reaction rate as a function of temperature T_9 is shown in Fig. 1. The dots represent results of the present calculations provided in Table I, while the continuous line represents its fitting by the function of T_9: $387.75 \times \left[1 + 0.5659T_9 - 0.052746T_9^2 + 0.0022354T_9^3\right]$. This yields a new reaction rate equation given by

$$\begin{aligned} N_{\rm A}\langle\sigma v\rangle &= (387.75 \pm 0.95) + (219.45 \pm 1.91)T_9 \\ &\quad -(20.45 \pm 0.59)T_9^2 + (0.867 \pm 0.045)T_9^3 \end{aligned} \tag{5}$$

expressed in units of $\mathrm{cm^3 s^{-1} mol^{-1}}$. When the direct capture effects are included, this rate equation gets modified to

$$\begin{aligned} N_{\rm A}\langle\sigma v\rangle &= (897.39 \pm 0.79) + (440.63 \pm 1.53)T_9 \\ &\quad -(46.36 \pm 0.46)T_9^2 + (1.753 \pm 0.035)T_9^3\,. \end{aligned} \tag{6}$$

As mentioned in the previous section, the TALYS code is not very suitable to obtain reliable results for a light system like ^{6}Li$(n,\gamma)^7$Li neutron radiative capture reaction cross sections. These can be reliably obtained from the Gamow shell model formulated in the coupled-channel representation [33] which at very low energies can be reasonably parametrized by the expansion

$$\sigma(E) = \frac{8.12828}{\sqrt{E}} - 0.496429 + 2.78499\sqrt{E}\,. \tag{7}$$

In Fig. 2, the calculated radiative neutron capture cross section for the reaction ^{6}Li$(n,\gamma)^7$Li has been plotted as a function of energy using the above equation and compared with the available experimental data [34–41]. Furthermore, using the above equation in Eq. (1) yields the reaction rate equation given by

$$N_{\rm A}\langle\sigma v\rangle = 1799391.963 \times \left(4.06414 - 0.08221833T_9^{1/2} + 0.179993902T_9\right)\,. \tag{8}$$

The plot of the above reaction rate as a function of T_9 is also shown in Fig. 3. As can be seen from Fig. 1, the reaction rate obtained from the TALYS calculation is largely underestimated for the reaction ^{6}Li$(n,\gamma)^7$Li. The reaction rates obtained in the present work, Eq. (8) and others as mentioned in Section 3, are meant to supersede the earlier reaction rates. When used in the BBN calculations by incorporating in the Kawano/Wagoner BBN code [32, 42, 43] modified by Singh *et al.* [31], the primordial elemental abundances, however, remained unchanged.

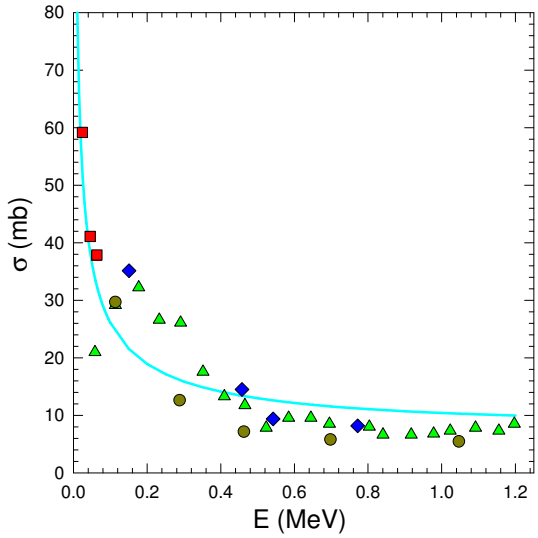

Fig. 2. The cross sections of the radiative neutron capture reaction $^{6}\mathrm{Li}(n,\gamma)^{7}\mathrm{Li}$ at low energies. The experimental results are from Refs. [34–41] and the line represents the theoretical calculations.

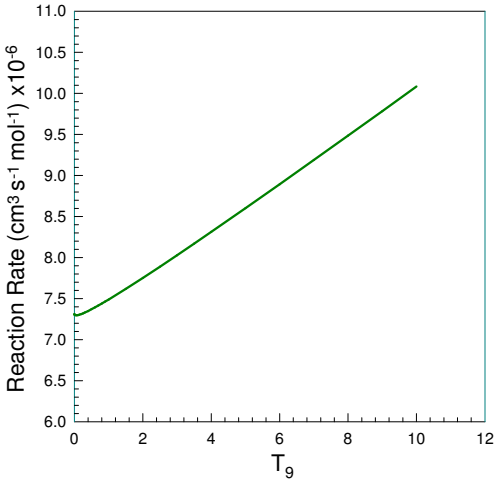

Fig. 3. Plot of reaction rate as a function of temperature T_9 obtained from the Gamow shell model formulated in the coupled-channel representation [33].

5. Conclusions

A new analytical expression for the thermonuclear reaction rate of ^{6}Li$(n,\gamma)^7$Li neutron capture reaction has been developed as a function of T_9. This has been achieved by fitting the results of the reaction rate generated from nuclear reaction theory calculations. Apart from the compound nuclear contribution, the pre-equilibrium and the direct effects have been accounted for. The thermonuclear reaction rate for ^{6}Li$(n,\gamma)^7$Li has been found to be temperature-dependent which increases monotonically beyond thermal neutron energies up to $10T_9$ that corresponds to ~ 0.86 MeV, while those for ^{10}B$(n,\gamma)^{11}$B, ^{12}C$(n,\gamma)^{13}$C and ^{14}N$(n,\gamma)^{15}$N remained constant within the same range of temperatures. Such a result implies that the compound nucleus picture is more or less true representation of slightly heavier nuclei such as ^{11}B, ^{13}C and ^{15}N. The primordial elemental abundances, however, remained unchanged when these new reaction rates have been used for it. This is expected as these reactions do not play any significant role in the standard Big Bang Nucleosynthesis because of the fact that there are little free neutrons available. Besides, in neutron-rich nucleosynthesis, the rate is too slow to compete with other reactions. Nevertheless, these new reaction rates may find usefulness in other domains of nuclear astrophysics such as stellar burning and stellar nucleosynthesis.

REFERENCES

[1] E.M. Burbidge, G.R. Burbidge, W.A. Fowler, F. Hoyle, «Synthesis of the Elements in Stars», *Rev. Mod. Phys.* **29**, 547 (1957).

[2] W.A. Fowler, F. Hoyle, «Neutrino Processes and Pair Formation in Massive Stars and Supernovae.», *Astrophys. J. Suppl.* **9**, 201 (1964), see Appendix C.

[3] D.D. Clayton, «Principles of Stellar Evolution and Nucleosynthesis», *University of Chicago Press*, Chicago 1983.

[4] J.C. Niemeyer, S.E. Woosley, «The Thermonuclear Explosion of Chandrasekhar Mass White Dwarfs», *Astrophys. J.* **475**, 740 (1997).

[5] P. Höflich, «Physics of type Ia supernovae», *Nucl. Phys. A* **777**, 579 (2006).

[6] T. Strohmayer, L. Bildsten, «New views of thermonuclear bursts», in: W.H.G. Lewin, M. Van der Klis (Eds.) «Compact Stellar X-ray Sources», *Cambridge University Press*, Cambridge 2006, p. 113.

[7] H. Schatz, L. Bildsten, A. Cumming, «Photodisintegration-triggered Nuclear Energy Release in Superbursts», *Astrophys. J.* **583**, L87 (2003).

[8] A. Cumming, J. Macbeth, J.J.M. in 't Zand, D. Page, «Long Type I X-Ray Bursts and Neutron Star Interior Physics», *Astrophys. J.* **646**, 429 (2006).

[9] S. Gupta *et al.*, «Heating in the Accreted Neutron Star Ocean: Implications for Superburst Ignition», *Astrophys. J.* **662**, 1188 (2007).

[10] E.G. Adelberger *et al.*, «Solar fusion cross sections. II. The *pp* chain and CNO cycles», *Rev. Mod. Phys.* **83**, 195 (2011).

[11] W.A. Fowler, G.R. Caughlan, B.A. Zimmerman, «Thermonuclear Reaction Rates», *Annu. Rev. Astron. Astrophys.* **5**, 525 (1967).

[12] R.N. Boyd, «An Introduction to Nuclear Astrophysics. 1st Ed.», *University of Chicago Press*, 2008.

[13] G.R. Caughlan, W.A. Fowler, «Thermonuclear reaction rates V», *Atom. Data Nucl. Data Tables* **40**, 283 (1988).

[14] R.A. Malaney, W.A. Fowler, «On nuclear reactions and 9Be production in inhomogeneous cosmologies», *Astrophys. J.* **345**, L5 (1989).

[15] M.S. Smith, L.H. Kawano, R.A. Malaney, «Experimental, Computational, and Observational Analysis of Primordial Nucleosynthesis», *Astrophys. J. Suppl.* **85**, 219 (1993).

[16] C. Angulo *et al.*, «A compilation of charged-particle induced thermonuclear reaction rates», *Nucl. Phys. A* **656**, 3 (1999).

[17] P. Descouvemont *et al.*, «Compilation and $\mathcal{R}$-matrix analysis of Big Bang nuclear reaction rates», *Atom. Data Nucl. Data Tables* **88**, 203 (2004).

[18] J.M. Blatt, V.F. Weisskopf, «Theoretical Nuclear Physics», *Springer-Verlag*, New York 1979.

[19] Tapan Mukhopadhyay, Joydev Lahiri, D.N. Basu, «Cross sections of neutron-induced reactions», *Phys. Rev. C* **82**, 044613 (2010); «Angular distributions of neutron–nucleus collisions», *ibid.* **83**, 067603 (2011).

[20] A.J. Koning, S. Hilaire, M.C. Duijvestijn, in: «Proceedings of the International Conference on Nuclear Data for Science and Technology, Nice, France, 22–27 April 2007», pp. 211–214; A. Koning, S. Hilaire, S. Goriely, TALYS-1.8 A nuclear reaction program, December 26, 2015.

[21] T. Rauscher, F.-K. Thielemann, K.-L. Kratz, «Nuclear level density and the determination of thermonuclear rates for astrophysics», *Phys. Rev. C* **56**, 1613 (1997).

[22] T. Rauscher, «Relevant energy ranges for astrophysical reaction rates», *Phys. Rev. C* **81**, 045807 (2010).

[23] T. Rauscher, F.-K. Thielemann, «Astrophysical Reaction Rates From Statistical Model Calculations», *Atom. Data Nucl. Data Tables* **75**, 1 (2000).

[24] T. Rauscher, F.-K. Thielemann, «Tables of Nuclear Cross Sections and Reaction Rates: An Addendum to the Paper "Astrophysical Reaction Rates From Statistical Model Calculations"», *Atom. Data Nucl. Data Tables* **79**, 47 (2001).

[25] W. Hauser, H. Feshbach, «The Inelastic Scattering of Neutrons», *Phys. Rev.* **87**, 366 (1952).

[26] J.A. Holmes, S.E. Woosley, W.A. Fowler, B.A. Zimmerman, «Tables of thermonuclear-reaction-rate data for neutron-induced reactions on heavy nuclei», *Atom. Data Nucl. Data Tables* **18**, 305 (1976).

[27] O. Toshiro *et al.*, «First measurement of neutron capture cross section of ^{6}Li at stellar energy», *AIP Conf. Proc.* **529**, 678 (2000).

[28] Su Jun *et al.*, «Neutron Spectroscopic Factors of ^{7}Li and Astrophysical ^{6}Li$(n,\gamma)^7$Li Reaction Rates», *Chin. Phys. Lett.* **27**, 052101 (2010).

[29] K.M. Nollett, M. Lemoine, D.N. Schramm, «Nuclear reaction rates and primordial ^{6}Li», *Phys. Rev. C* **56**, 1144 (1997).

[30] K.M. Nollett, S. Burles, «Estimating reaction rates and uncertainties for primordial nucleosynthesis», *Phys. Rev. D* **61**, 123505 (2000).

[31] Vinay Singh, Joydev Lahiri, Debasis Bhowmick, D.N. Basu, «Big-Bang Nucleosynthesis and Primordial Lithium Abundance Problem», *J. Exp. Theor. Phys.* **128**, 707 (2019); *ibid.* **155**, 832 (2019).

[32] R. Wagoner, «Synthesis of the Elements Within Objects Exploding from Very High Temperatures», *Astrophys. J. Supp.* **18**, 247 (1969).

[33] G.X. Dong *et al.*, «Gamow shell model description of radiative capture reactions ^{6}Li$(p,\gamma)^7$Be and ^{6}Li$(n,\gamma)^7$Li», *J. Phys. G: Nucl. Part. Phys.* **44**, 045201 (2017).

[34] G.A. Bartholomew, P.J. Campion, «Neutron Capture Gamma Rays from Lithium, Boron, and Nitrogen», *Can. J. Phys.* **35**, 1347 (1957).

[35] L. Jarczyk *et al.*, «(n,γ)-Spektren und Wirkungsquerschnitte von Lithium, Beryllium und Kohlenstoff», *Helv. Phys. Acta* **34**, 483 (1961).

[36] E.T. Jurney, «Thermal capture cross sections for ^{6}Li and ^{7}Li», *U.S. Nucl. Data Comm.* **9**, 109 (1973).

[37] C.S. Park, G.M. Sun, H.D. Choi, «Determination of thermal neutron radiative capture cross section of ^{6}Li», *Nucl. Instrum. Methods Phys. Res. B* **245**, 367 (2006).

[38] T. Ohsaki *et al.*, «First measurement of neutron capture cross section of ^{6}Li at stellar energy», *AIP Conf. Proc.* **529**, 678 (2000).

[39] S. Karataglidis *et al.*, «The ^{7}Li$(\gamma,n_0)^6$Li cross section near threshold», *Nucl. Phys. A* **501**, 108 (1989).

[40] R.L. Bramblett *et al.*, «Systematic properties of the giant resonance: current status», *Proc. Int. Conf. Photonucl. React. Appl. California* **1**, 175 (1973).

[41] L. Green, D.J. Donahue, «Photoneutron Cross Sections With Monoenergetic Neutron-Capture Gamma Rays», *Phys. Rev.* **135**, B701 (1964).

[42] R. Wagoner, W.A. Fowler, F. Hoyle, «On the Synthesis of Elements at Very High Temperatures», *Astrophys. J.* **148**, 3 (1967).

[43] L. Kawano, FERMILAB Report No. PUB-92/04-A, January 1992 (unpublished).